

## Redox and ATP control of photosynthetic cyclic electron flow in *Chlamydomonas reinhardtii* (I) aerobic conditions

Jean Alric<sup>a,\*</sup>, Jérôme Lavergne<sup>b</sup>, Fabrice Rappaport<sup>a</sup>

<sup>a</sup> UMR 7141, CNRS et Université Pierre et Marie Curie (Paris VI), Institut de Biologie Physico-Chimique, 13 rue Pierre et Marie Curie 75005 Paris, France

<sup>b</sup> DSV/IBEB/SBVME/LBC, UMR 6191, CNRS/CEA/Univ. Aix-Marseille II, CEA Cadarache, 13108 Saint Paul lez Durance, France

### ARTICLE INFO

#### Article history:

Received 17 April 2009

Received in revised form 22 July 2009

Accepted 24 July 2009

Available online 3 August 2009

#### Keywords:

Electron transfer

Green algae

*Chlamydomonas reinhardtii*

Photosystem I

Cytochrome *b<sub>6</sub>f*

### ABSTRACT

Assimilation of atmospheric CO<sub>2</sub> by photosynthetic organisms such as plants, cyanobacteria and green algae, requires the production of ATP and NADPH in a ratio of 3:2. The oxygenic photosynthetic chain can function following two different modes: the linear electron flow which produces reducing power and ATP, and the cyclic electron flow which only produces ATP. Some regulation between the linear and cyclic flows is required for adjusting the stoichiometric production of high-energy bonds and reducing power. Here we explore, in the green alga *Chlamydomonas reinhardtii*, the onset of the cyclic electron flow during a continuous illumination under aerobic conditions. In mutants devoid of Rubisco or ATPase, where the reducing power cannot be used for carbon fixation, we observed a stimulation of the cyclic electron flow. The present data show that the cyclic electron flow can operate under aerobic conditions and support a simple competition model where the excess reducing power is recycled to match the demand for ATP.

© 2009 Elsevier B.V. All rights reserved.

### 1. Introduction

Whereas photosynthetic prokaryotes such as purple bacteria or green sulfur bacteria and heliobacteria possess only one photosynthetic reaction center (type II or I), chloroplasts and cyanobacteria have both photosystems. Type II reaction centers transfer electrons to the quinone pool. In purple bacteria, the cytochrome *b<sub>c</sub>1* complex recycles these electrons, *via* periplasmic electron carriers (mostly cytochromes), towards the photo-oxidized primary electron donor. This cyclic process results in the building of a membrane potential which drives ATP synthesis. On the other hand, green sulfur bacteria and heliobacteria oxidize sulfur reduced compounds to generate secondary electron donors to their type I reaction center which in turn produces reducing power (NADH). In cyanobacteria, green algae and plants these two photosynthetic units are coupled to drive the reduction, by photosystem I (PSI), of a terminal electron acceptor NADP<sup>+</sup>, at the expense of a ubiquitous primary electron donor, water, oxidized by photosystem II (PSII). The unique photochemistry of water oxidation is carried out at the donor (lumenal) side of PSII by the oxygen evolving complex.

At variance with the ancestral type II reaction center, photosystem II is thus no longer capable of accepting electrons released in the lumen

by the cytochrome *b<sub>6</sub>f*, and thus incapable of participating to a cyclic electron flow involving the *b<sub>6</sub>f* complex and a soluble electron carrier.

In a strictly linear electron transfer from water to NADP<sup>+</sup>, ATP and NADPH are produced in a ratio of 9:7, but carbon fixation in the Calvin–Benson–Bassham cycle (hereafter called Calvin cycle) requires 3 ATP per 2 NADPH molecules, *i.e.* a ratio of 9:6 (for a review, see [1]). Furthermore, many other cellular processes require ATP, such as the carbon-concentrating mechanism found in *Chlamydomonas* [2], and this further unbalances the ATP to NADPH ratio with respect to the stoichiometric requirements of the Calvin cycle. Several mechanisms may be considered, that may adjust the production of high-energy bonds and reducing power to the demand of carbon fixation. One possibility is to dissipate part of the reducing power *via* electron transfer towards molecular oxygen (Mehler reaction [3], or Plastid Terminal Oxidase activity [4,5], located on the stromal side of the thylakoid membrane [6] and shown in orange in Fig. 1). These reactions directly or indirectly oxidize the quinol molecules produced by PSII, and therefore participate to the formation of a proton-motive force at the level of the thylakoid membrane, and drive ATP synthesis. Another way would be to export the excess reducing power towards mitochondria *via* the malate valve [7] (see Fig. 1). In the latter case, electrons end up on O<sub>2</sub> as well, and, so doing, promote ATP synthesis in the mitochondrion. Under certain circumstances, this mitochondrial ATP could be used for carbon fixation [8].

However, the question as to whether the shuttle of metabolites between organelles is fast enough to compete with linear electron flow remains open, and several models have been proposed according to which the additional ATP would be produced, not via the mitochondria, but directly at the level of the thylakoid membrane by cyclic electron flow involving PSI (see [1] for a review). Two models presently prevail.

**Abbreviations:** PSII, photosystem II; PSI, photosystem I; P<sub>700</sub>, primary electron donor of PSI (reduced form); P<sub>700</sub><sup>+</sup>, primary electron donor of PSI (oxidized form); DCMU, 3-(3,4-dichlorophenyl)-1,1-dimethylurea; HA, hydroxylamine; DBMB, 2,5-dibromo-3-methyl-6-isopropyl-*p*-benzoquinone; MV, methylviologen

\* Corresponding author.

E-mail address: [jean.alric@ibpc.fr](mailto:jean.alric@ibpc.fr) (J. Alric).

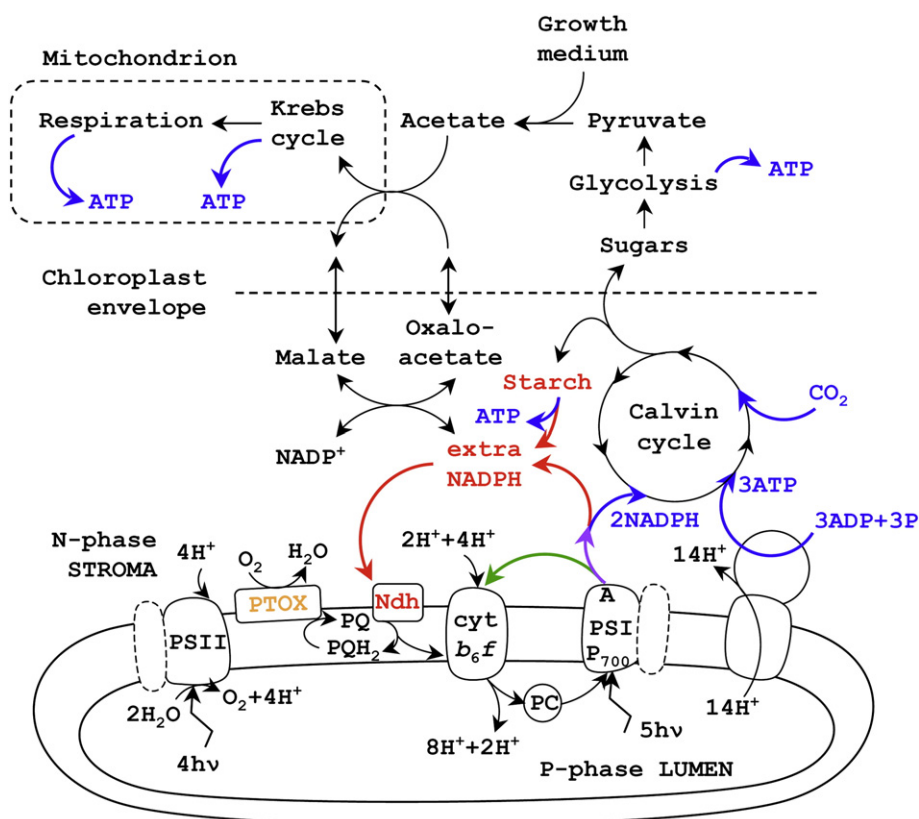


**Fig. 1.** Schematic representation of the electron transfer pathways in the chloroplast. The requirement for 3 ATP per 2 NADPH molecules to drive the Calvin cycle can be met if 1 electron in 9 is recycled, the other 8 being transferred linearly through 4 turnovers of PSII and PSI for the storage of 2 NADPH molecules (see [1]). The figure of 5 PSI turnovers accounts for these 4 electrons transferred to NADPH together with the additional cyclic turnover.

The first (historical) one states that Ferredoxin (Fd) is able to donate electrons to the cytochrome  $b_6f$  [9] (shown in green in Fig. 1). This model involves less molecular intermediates than others, and it also fits with the original scheme of the Mitchellican Q-cycle, where the electron transfer reactions at both sides of the membrane are symmetric, and quinones play the role of catalysts [10,11]. The second type of models arose from molecular biology and biochemical studies. They involve a respiratory-type NADPH dehydrogenase (shown in red in Fig. 1, for a review, see [12]) which transfers electrons into the quinone pool. This latter electron transfer pathway certainly occurs in prokaryotes (green sulfur bacteria, heliobacteria and cyanobacteria) since the photosynthetic and respiratory chains share the same membrane. In eukaryotes, the photosynthetic and respiratory chains are segregated into separate organelles (chloroplast and mitochondrion). Nevertheless, the conservation of multiple respiratory-type enzymes in the chloroplast of eukaryotes (green algae [13] and plants [14]), does suggest that a respiratory-type activity may be coupled to the photosynthetic activity.

In this paper, three main results are shown: (i) in *Chlamydomonas reinhardtii*, the onset of cyclic electron flow is observed after 1 s of illumination; (ii) the comparison of the WT with mutants inactivated for the Calvin cycle provides support to the view that cyclic electron flow is mainly controlled by the redox poise of the stroma [15]; (iii) a specificity of green algae, when compared to plants, is to mobilize efficiently their reserves in the dark, injecting reducing power into the chloroplast.

## 2. Experimental procedures

### 2.1. Strains of *Chlamydomonas reinhardtii* and growth conditions

Wild type (WT) cells, ATPase depleted cells (Fud50, [16]), the strain without Rubisco was a kind gift of Spreitzer (31.4E, [17,18]), or

cells devoid of cytochrome  $b_6f$  complex ( $\Delta petD$ , [19]) were grown at 25 °C in photoheterotrophic conditions (Tris/Acetate/Phosphate (TAP) medium and light irradiance of 300 lux). In exponential phase, cells were harvested by centrifugation at 4000g for 5 min and resuspended in HEPES 20 mM pH 7.2 plus Ficoll 20% to obtain a final concentration of photosystem I of approximately 100 nM, estimated from absorbance changes at 700 nm (see below). Although resuspended in buffer, the cells were not washed free from acetate (depletion of acetate in the medium would have required 4 h of starvation in minimum buffer as described in [20]). Inhibitors were purchased from Sigma. In almost all the data presented in this article, Hydroxylamine (HA) 1 mM and 3-(3,4-dichlorophenyl)-1,1-dimethylurea (Diuron, or DCMU) 10  $\mu$ M were added to block electron transport in PSII. 2,5-dibromo-3-methyl-6-isopropyl-*p*-benzoquinone (DBMIB) 20  $\mu$ M, inhibitor of the  $Q_0$  site of the cytochrome  $b_6f$  complex, was used to evaluate the total amount of  $P_{700}$ . Methylviologen (MV) 10 mM was used as an efficient PSI electron acceptor.

### 2.2. Optical spectroscopy

Light-induced absorbance changes were measured as previously described in the supplementary material of reference [21], with a JTS 10 (BioLogic) spectrophotometer equipped with light emitting diodes (LEDs). This spectrophotometer has an excellent signal/noise ratio which renders averaging unnecessary and allows the observation of prolonged dark-adapted states. Absorbance changes due to  $P_{700}$  were probed with a measuring beam consisting of short pulses of about 10  $\mu$ s time-duration, provided by a pulsed LED peaking at 700 nm, and filtered through a 10 nm bandwidth interference filter centered at 705 nm. Long-pass 3 mm thick RG695 Schott colored glass filters were placed in front of the detectors (silicon photodiodes with preamplifiers)

to reject most of the light excitation provided by a powerful LED emitting in the 620 nm region. This continuous red actinic illumination of 10 s was hatched by very short (200  $\mu$ s) dark intervals, during which were delivered, at 150  $\mu$ s, the 10  $\mu$ s detecting pulses. This short delay, between the cessation of illumination and the probe of absorbance, is greater than the time-constant of the detectors (about 10  $\mu$ s) but smaller than the long-lived  $P_{700}^+$  signal, accumulated in the light ( $t_{1/2} \sim 100$  ms, see the Results section). A digital pulse generator allows the programming of these complex measurement sequences. After a baseline drawn in the dark, the kinetics of  $P_{700}$  oxidation were recorded in the light during 10 s, and the dark recovery of  $P_{700}$  reduction was also measured.

We cannot exclude that, when detecting the absorption changes at 705 nm, some PSII fluorescence excited by the probe pulse is also present. This contribution is certainly small, but changes of the PSII fluorescence yield could cause some distortion to our measurements. That is the reason why we systematically added HA when we used DCMU (except in the experiments shown in Fig. 2). In the presence of these donor side (HA) and acceptor side (DCMU) inhibitors, PSII remains blocked in the closed (high fluorescence state) following an initial preillumination.

### 3. Results

The illumination of a chain of photosynthetic redox compounds leads, after a sufficient period of time (a few seconds in most cases), to a steady-state regime which depends on the light intensity. In other words, for any carrier within the chain, the concentration of its reduced (or oxidized) form does not change with time, i.e. the reduction rate of this carrier is equal to its oxidation rate [22]. Maxwell and Biggins [23] used this

principle when following  $P_{700}$  redox changes: when a steady-state level of  $P_{700}^+$  is accumulated in the light, the electron flow rate through PSI is equal to the reduction flow rate of  $P_{700}^+$  measured after cessation of illumination.

When linear electron flow is eliminated, either by PSII inhibition with DCMU or by using light excitation specific to PSI, one can isolate the cyclic electron flow. From our experience with *Chlamydomonas reinhardtii* cells, and in contrast with higher plants (see [21] for a recent example), it is not possible to use far red light (>720 nm) for this purpose. We found that  $P_{700}$  is hardly oxidized by such light in *Chlamydomonas*, probably because of the weaker far red absorption bands in PSI-LHCI complexes when compared to higher plants [24]. We therefore used DCMU to inhibit linear electron flow.

Under anaerobic conditions the intracellular redox poise becomes more reducing as a result of the halt of the respiratory chain. We observed that this may lead to an increased probability for charge recombination between the reduced PSI electron acceptors and  $P_{700}^+$ , leading to a possible overestimation of the cyclic electron flow rate when derived from the  $P_{700}^+$  reduction rate. This problem does not arise under aerobic conditions as in the present study.

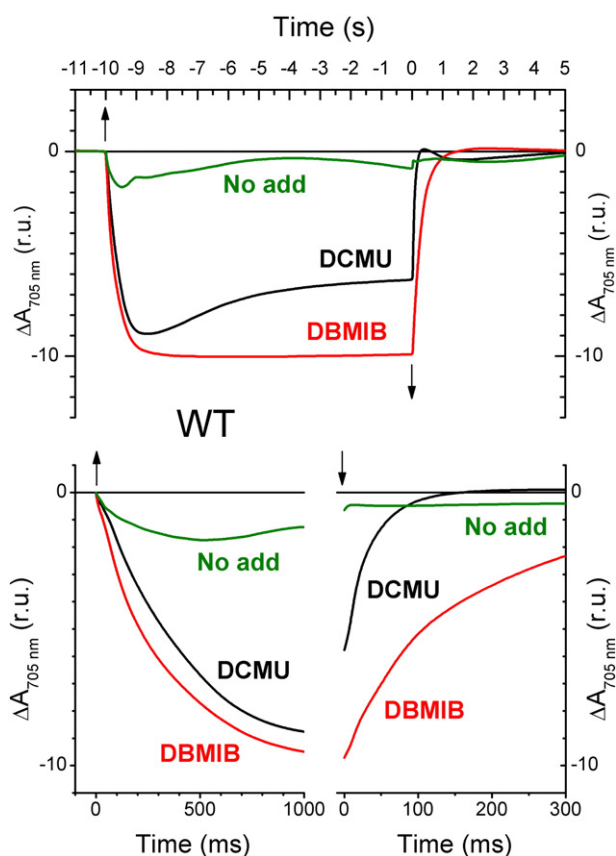
#### 3.1. Intersystem, cyclic and inhibited electron flow

Fig. 2 exemplifies how  $P_{700}$  oxidation–reduction kinetics probe the photosynthetic activity. Under a light intensity of approximately  $50 \mu\text{E m}^{-2} \text{s}^{-1}$ , which led to an initial photochemical rate of about 50 electrons transferred per PSI per second, and in the absence of inhibitors, little accumulation of oxidized  $P_{700}^+$  was observed. In this case, the intersystem electron transfer is faster than the photochemical rate and the electrons, produced at the donor side of PSII, are transferred to PSI. However, illumination at the same light intensity induced the oxidation of  $P_{700}$  to a significant extent when PSII or the  $b_6f$  complex was blocked by DCMU or DBMIB, respectively. These results show that the 620 nm red light used for the excitation of the sample is absorbed by both photosystems.

Let us now examine the kinetics obtained in the presence of DBMIB, an inhibitor of the site  $Q_o$  of the cytochrome  $b_6f$  complex. Under such conditions, the electron transfer from the quinone pool to  $P_{700}$  is expected to be markedly slowed down. And, indeed, DBMIB addition (Fig. 2) resulted in a monotonous oxidation of  $P_{700}$  in the light. Increasing concentrations of DBMIB (not shown) did not change much the steady-state level of  $P_{700}^+$  (maximum extent of  $P_{700}^+$ ) but decreased the initial slope of the dark-recovery after cessation of illumination. This rate is thus mainly controlled by the electron flux through the  $Q_o$  site of cyt  $b_6f$  complex, and is hardly contributed by other processes such as charge recombination between the reduced PSI electron acceptors ( $A^-$ ) and  $P_{700}^+$ .

In the presence of DCMU, PSII is inhibited and the overall linear electron flow (from water to  $\text{CO}_2$ ) is blocked. Under such conditions, however, a transient “pseudo-linear” electron transfer, from PSI secondary electron donors (two PC, one cyt  $f$ , one Rieske and few  $\text{PQH}_2$  per PSI) to PSI electron acceptors ( $\text{NADP}^+$ , FNR, Fd), can still occur in the first several hundred milliseconds of illumination. In this time-range, roughly similar time courses of  $P_{700}$  oxidation were observed in the presence of DCMU or of DBMIB. The kinetics were however somewhat slower in the presence of DCMU, which is consistent with the presence of a few  $\text{PQH}_2$  in the dark-adapted state, which contribute to the stock of reduced electron donors to  $P_{700}$  in the presence of DCMU, but not when the  $b_6f$  complex is inhibited by DBMIB.

At later times (>1 s), the kinetics became divergent. In the presence of DCMU, a remarkable overshoot appeared, whereupon a steady-state was reached at an intermediate level of  $P_{700}$  oxidation. When the light was turned off at 10 s, the signal relaxed rapidly with a rate of about  $10 \text{ s}^{-1}$  (see Fig. 2, bottom right panel). This overshoot was not observed in the presence of DBMIB, irrespective of the presence of DCMU.



**Fig. 2.** Effect of DCMU (10  $\mu\text{M}$ ) and DBMIB (20  $\mu\text{M}$ ) on the kinetics of  $P_{700}$  oxidation–reduction, followed at 705 nm and induced by a 10 s duration illumination in WT algae. Upward and downward arrows mark the moments when the light is switched on and off, respectively. The uppermost panel shows the whole kinetics, while underneath are detailed the kinetics at the switch on (left) and off (right).

From a kinetic point of view, the main result is that  $P_{700}^+$  is accumulated in the presence of DCMU whereas it is not in the absence of inhibitors. This simply shows that, in the present conditions, the cyclic flow is slower than linear (or intersystem) flow, and that the two regimes have different limiting steps. The limiting step for cyclic electron flow is not the quinol oxidation at the  $Q_o$  site of the cytochrome  $b_6f$ , as it is for linear electron flow, but rather an upstream step of electron transfer, very likely from the stroma to the PQ pool.

### 3.2. Activation and deactivation of cyclic electron flow

We will now address the issue raised by the observation of an overshoot in the  $P_{700}$  oxidation kinetics. Since the redox state of  $P_{700}^+$  is expected to be a function of its oxidation and reduction rates, and the former being constant (continuous illumination), the overshoot may witness a variation in the reduction rate. This hypothesis was tested by measuring this rate at the time corresponding to the maximum of the overshoot (Fig. 3). When the light is switched off when the amplitude of  $P_{700}^+$  is maximum (at 2 s in Fig. 3), its dark recovery kinetics is about twice slower (about  $3\text{ s}^{-1}$ ) than after activation of cyclic electron flow (about  $7\text{ s}^{-1}$ , at 10 s in Fig. 3). This observation clearly shows that the cyclic electron flow rate varies during the illumination.

### 3.3. Factors influencing the rate of cyclic electron flow

In the dark-adapted state,  $P_{700}$  and its secondary donors ( $\sim 2$  PCs, one Rieske, one cyt  $f$  and few  $PQH_2$  per PSI) are reduced whereas PSI secondary electron acceptors are essentially oxidized. In the light,  $P_{700}^+$  is accumulated, which implies that its secondary donors (of lower midpoint potential) are also oxidized. Thus, throughout the duration

of the illumination, at least 5–10 electrons are transferred from the lumen to the stroma. These electrons can follow two possible pathways: the Calvin cycle or cyclic electron flow (we neglect electron backflow or charge recombination in PSI, and the Mehler reaction). In order to discriminate these different pathways we have studied mutants in which the Calvin cycle is ineffective, a mutant devoid of Rubisco and a mutant lacking ATPase. The data, obtained with various light intensities, are presented in Fig. 4.

Under low light intensities, a lag in the  $P_{700}$  oxidation kinetics was observed in the few hundreds of milliseconds after the onset of the illumination. The duration of the lag, which depends on the light intensity (see red and black curves in Fig. 4), reflects the time needed to oxidize the PSI secondary electron donors which were reduced in the dark: PC, cyt  $f$ , Rieske and few quinones. It thus provides a measure of the redox state of the electron transfer chain upstream of PSI. This lag was identical in the strains studied here, showing that the lack of Rubisco or ATP synthase did not result in a significant change of the redox state of the PQ pool. The overshoot at 1–2 s of illumination was absent in the  $b_6f$ -depleted strain (Fig. 4D, as it was in the sample treated with DBMIB, see Fig. 2). On the other hand it was less pronounced in the WT (Fig. 4A) than in the strains inactivated for the carboxylase (Fig. 4B) or the ATPase (Fig. 4C). For the same initial photochemical rate, for example see the red curves in Fig. 4, the steady-state level of  $P_{700}^+$  at 10 s was larger in the mutant devoid of cyt  $b_6f$  than in the WT, and smaller in the mutants devoid of carboxylase or ATPase. This means that cyclic electron flow is almost inactive in the absence of cyt  $b_6f$ , and stimulated in the absence of Rubisco or ATPase. These changes can also be characterized based on the dark recovery kinetics of  $P_{700}$ , for example when its full oxidation was induced by a saturating light intensity (purple curves). For better visualization, these post-illumination kinetics are shown in Fig. 5.

The dark recovery kinetics of  $P_{700}$  are nicely fitted to a first order model, which allows the determination of accurate rate constants. The absence of cytochrome  $b_6f$  slows down the electron transfer towards  $P_{700}^+$  to about  $1\text{ s}^{-1}$  (this reduction rate may originate from electron backflow or charge recombinations within PSI) whereas the absence of Rubisco or ATPase results in a two-fold increase of this electron transfer rate, from about 8–10  $\text{s}^{-1}$  in the WT to 14–15  $\text{s}^{-1}$  in the mutants.

The faster re-reduction rate of  $P_{700}$  in the mutants is specific to light conditions and does not reflect a more reduced state of the intersystem pool in the dark (as could be caused, e.g. by an increased Ndh activity in the mutants). Indeed, the state of this pool appears unaltered in the mutants, as can be inferred from the similar duration of the lag mentioned above, or from a test using fluorescence induction (see Fig. S1 in Supplementary Material). The increased rate of the cyclic flow in the mutants is therefore due to an increased pressure of reduced equivalents at the acceptor side of PSI, which results from the inactivation of the Calvin cycle in the Rubisco- or ATPase-less mutants. Under all likelihood, such a modulation of the cyclic electron flow is also at work in the WT whenever the ATP content does not meet the Calvin requirement. As in the ATPase-less or Rubisco-less mutants described here, this would imbalance the rates of NADPH production and consumption. Such disequilibrium results in the WT in a progressive increase of the NADPH pool, and is compensated by an enhancement of the cyclic flow, proton translocation and ATP synthesis.

In Fig. 6, we have plotted the dark recovery kinetics of  $P_{700}$  after various durations of illumination in the range of minutes. Under such conditions, the baseline is taken in the light and the recovery of  $P_{700}$  is measured after cessation of illumination ( $t=0$ ). The rate constant varied from  $8\text{ s}^{-1}$  after 10 s of illumination (see Fig. 5) to  $4\text{ s}^{-1}$  after 60 s of illumination, then gradually increased to a maximum value of about  $10\text{ s}^{-1}$  at 10 min and decreased again when prolonging further the illumination. In Fig. 6, the zero of the vertical scale is the steady-state level reached in the light, which corresponds to different amounts of oxidized  $P_{700}$ , as can be seen from the amplitudes of the

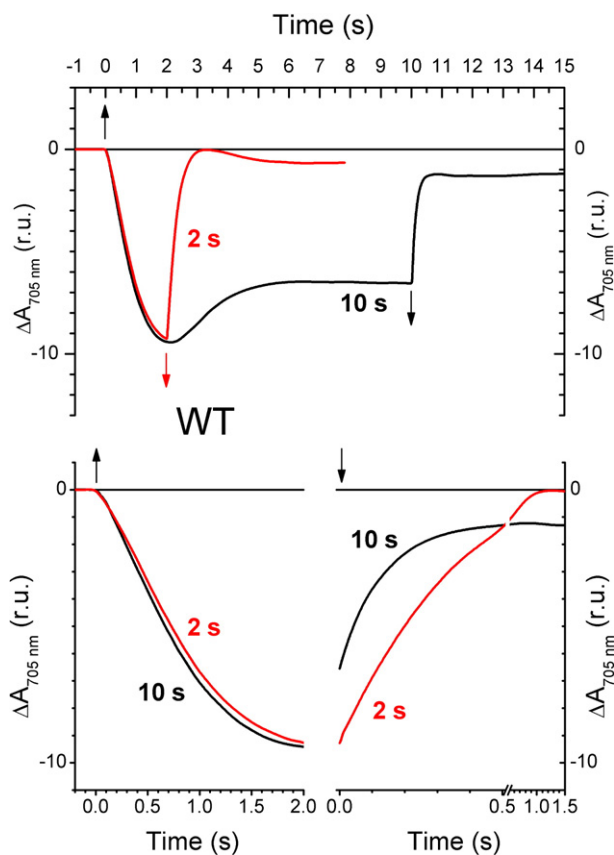


**Fig. 3.** Effect of the light duration on the kinetics of  $P_{700}^+$  reduction in the dark, followed at 705 nm and induced by a 2 s or 10 s light pulse in WT algae treated with 10  $\mu\text{M}$  DCMU. In this experiment and those shown in subsequent figures, HA (1 mM) was present.



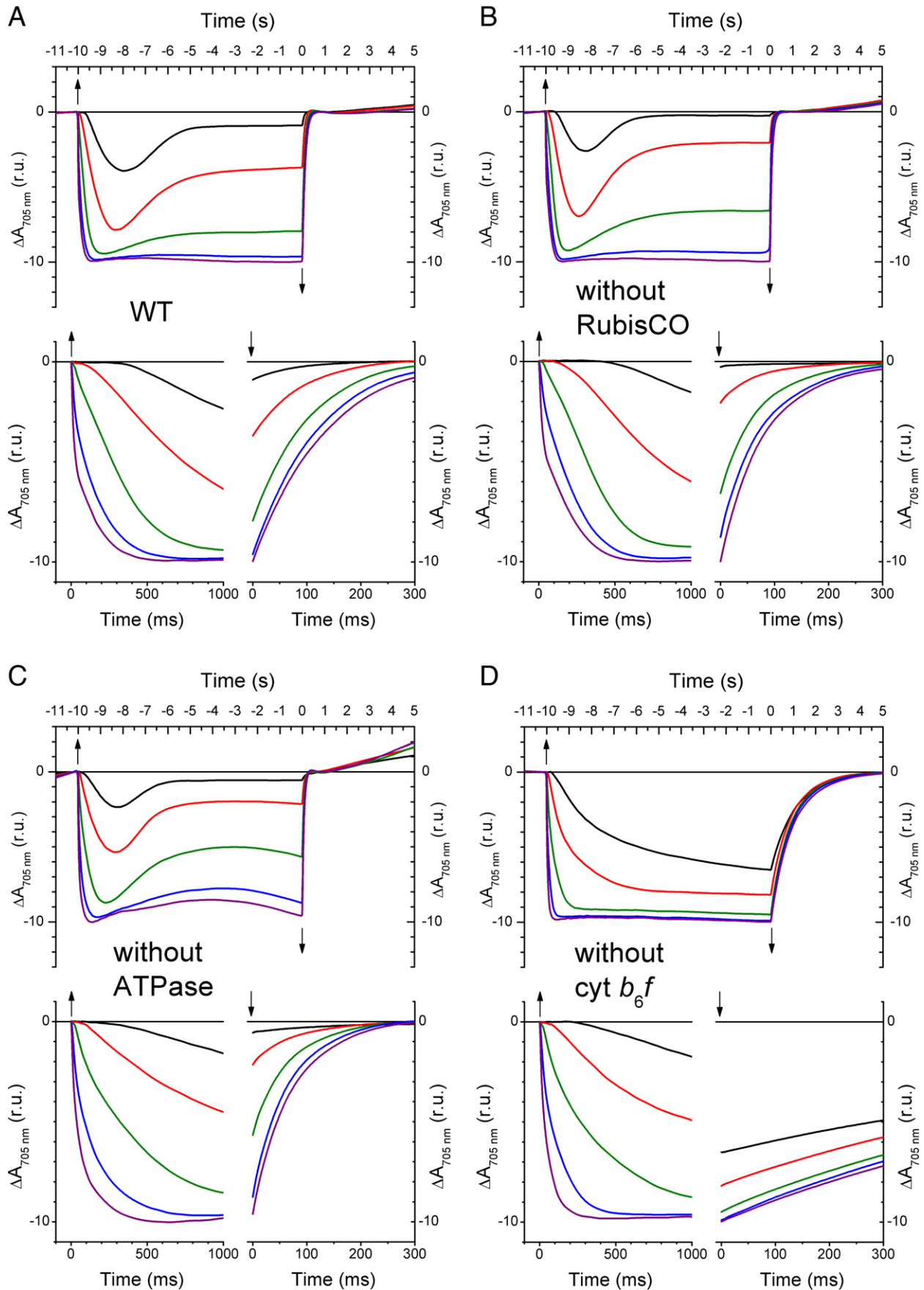


**Fig. 4.** Survey of various mutations and their functional consequences on  $P_{700}$  kinetics. Same conditions as in Fig. 3. The light intensity was approximately  $5 \mu\text{E m}^{-2} \text{s}^{-1}$  (black),  $20 \mu\text{E m}^{-2} \text{s}^{-1}$  (red),  $50 \mu\text{E m}^{-2} \text{s}^{-1}$  (green),  $200 \mu\text{E m}^{-2} \text{s}^{-1}$  (blue),  $500 \mu\text{E m}^{-2} \text{s}^{-1}$  (purple). The figure is split into four main panels corresponding to the WT (A), and three strains inactivated for Rubisco (B), chloroplast ATPase (C) or cytochrome  $b_6f$  (D) assembly, as indicated.

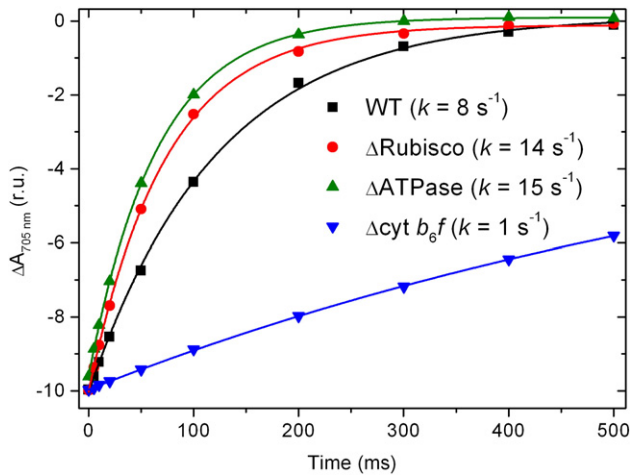


**Fig. 5.** First order dark recovery kinetics of  $P_{700}$  in the various mutant strains after 10 s of saturating light. Data are taken from Fig. 4, purple curves (saturating light). The data were fitted to an exponential decay.

reduction kinetics. This variable extent of  $P_{700}^+$  under non saturating illumination appears simply correlated with the reduction rate in the dark (as observed above in the experiments of Figs. 3 and 4): the faster the rate, the smaller the fraction of oxidized  $P_{700}$ .

The reasons underlying the changes in the reduction rate of  $P_{700}^+$  after various periods of illumination are unknown, but they presumably reflect modifications in the amount of stromal reductants, caused by a modulation of the Calvin cycle activity. In agreement with this view, the reduction rate did not depend on the illumination duration in the mutants lacking Rubisco or ATPase (see Fig. S2 in Supplementary Material).

### 3.4. Shunting the electron flow towards methylviologen

Methylviologen (MV) is an efficient PSI electron acceptor that bypasses the electron transfer towards NADPH, because of its lower midpoint potential (by ~100 mV) and the rapid reaction of its reduced radical with  $O_2$ . In the presence of DCMU, when increasing concentrations of MV were added, the reduction of  $P_{700}^+$  in the dark was progressively slowed down (not shown), until a saturating concentration (of 3 mM) is reached, after which  $P_{700}^+$  reduction rate was stabilized to ~2–3  $s^{-1}$  (see Fig. 7).

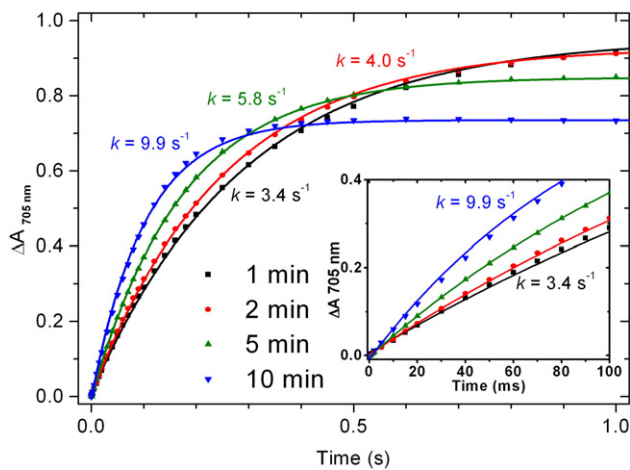


**Fig. 6.** Dark recovery kinetics of  $P_{700}$  during adaptation in the light. The data were measured in the WT strain and fitted to an exponential decay. A continuous light was applied during the entire period of the experiment, lasting several minutes, and the decay of  $P_{700}$  was measured from time to time during 1 s dark intervals.

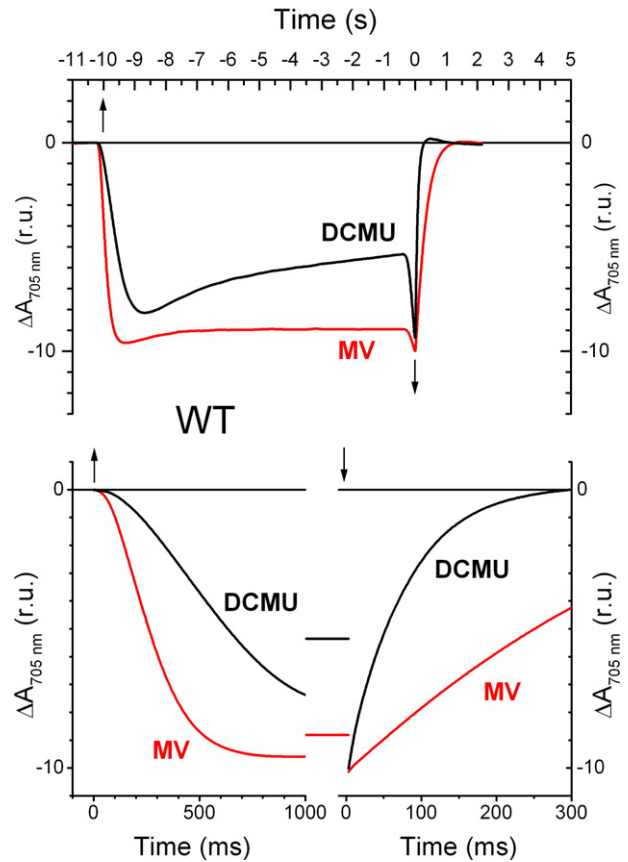


**Fig. 7.** Effect of 10 mM methylviologen (MV) on  $P_{700}$  oxidation–reduction kinetics measured in the presence of DCMU. The light intensity was about  $50 \mu E m^{-2} s^{-1}$  and a saturating pulse of 200 ms was applied at the end of the illumination period to reach the full extent of  $P_{700}^+$ .

Thus, although the electron flow rate towards  $P_{700}^+$  is significantly decreased by MV, it is still about 2-fold faster than in the  $cyt b_6f$ -depleted mutant. The overshoot in the  $P_{700}$  kinetics is largely diminished, but not totally eliminated by MV.

## 4. Discussion

In this work we have estimated the cyclic electron flow in *Chlamydomonas reinhardtii* under aerobic conditions, by following the oxidation and reduction state of  $P_{700}$  within the PSI complex, while PSII was inactivated by DCMU. The flow rate ( $F$ , in electrons transferred per second per PSI,  $e^- s^{-1} \cdot PSI^{-1}$ ) or the PSI turnover (in  $e^- s^{-1}$ ) can be easily determined from the reduction rate constant ( $k$ , in  $s^{-1}$ ) of  $P_{700}^+$  after switching the illumination off, knowing the relative concentration  $[P_{700}^+]$  under steady-state illumination, as:  $F = k [P_{700}^+]$ . When a saturating light is used,  $P_{700}$  is fully oxidized ( $[P_{700}^+] = 1$ ) and the flow rate is equal to the reduction rate ( $F = k$ ).

We have shown that in the absence of the cytochrome  $b_6f$  complex, the flow is very low (~1  $e^- s^{-1} \cdot PSI^{-1}$ ), whereas it is about ten-fold faster in its presence. This provides evidence for a sustained cyclic electron transport around PSI involving electron transfer through  $cyt b_6f$  and thus promoting proton translocation and ATP synthesis.

### 4.1. Mechanism of sustained cyclic electron flow

Our results show a difference in the flow rate between the WT (~10  $e^- s^{-1} \cdot PSI^{-1}$ ) and the mutants inactivated for Rubisco or ATPase (~15  $e^- s^{-1} \cdot PSI^{-1}$ ). This indicates that, although PSII was inhibited by DCMU, the Calvin cycle was active, at least partially, in the WT, since it affects the amount of electrons that can be allocated to cyclic transfer.

One may reason that, being active, the Calvin cycle should exhaust the limited stock of electrons present in the dark in PSI secondary donors (2 PCs, 1 cyt *f*, 1 Rieske protein, and ~2 PQH<sub>2</sub> in aerobic conditions) and eventually lead to the complete oxidation of P<sub>700</sub><sup>+</sup>. At variance with this prediction, a steady-state cyclic flow remained after rather long illumination durations (see e.g. Fig. 6). Thus an entry of electrons into the system must compensate for their consumption by the Calvin cycle. This conclusion is further supported by the finding that in the presence of MV, which acts as an electron sink and thus competes with the reinjection of electrons into the chain *via* the cyclic process, a small but significant fraction of P<sub>700</sub><sup>+</sup> remained reduced. Also consistent with this, Bulté et al. reported a significant light-induced ATP synthesis in the presence of MV and in the absence of PSII activity [25]. Based on the reduction rate of P<sub>700</sub><sup>+</sup> in the presence of MV, we estimate this electron influx to 2–3 e<sup>-</sup> PS<sup>-1</sup>. We propose that this influx compensates for the escape of electrons *via* the Calvin cycle, and quantitatively account for the difference observed between the WT and the mutants in which CO<sub>2</sub> reduction cannot take place.

In addition, the faster rate observed in the mutants lacking Rubisco or ATPase also provide insight into the parameters which control the cyclic electron flow rate. In these mutants we observe a “pure” cyclic flow, since no electrons can escape the cycle. A larger accumulation of reduced equivalents in the stroma ensues. The cyclic electron flow around PSI being faster in such conditions, one may conclude that its rate is primarily controlled by the redox state of the stromal electron acceptors, as proposed by Arnon and Chain [15]. Accordingly, the reduction level of NADPH, and thus the cyclic flow rate, are expected to be larger under conditions where PSII is at work and injects electrons into the chain, especially under anaerobic conditions. This should be qualified, however, since the accumulation of reducing power in PSI acceptors may also cause charge recombination within PSI [26] and this non productive cyclic pathway might also contribute to accelerate P<sub>700</sub><sup>+</sup> reduction.

We propose that, on the one hand, a significant fraction of the reducing power produced by PSI is allocated to the Calvin cycle, even in the absence of PSII activity, and, on the other hand, that this electron efflux is compensated by an influx. This raises the question of the origin of this electron influx and of the possible adjustment of the various fluxes during the illumination. In the dark, as discussed in [25] the plastoquinone pool undergoes an influx of electrons resulting from carbohydrates catabolism and the chlororespiratory oxidase consumes these electrons keeping the plastoquinone pool mostly oxidized [5]. The carbohydrate catabolism although most likely mainly directed towards the mitochondrion, also exerts a reductive pressure in the chloroplast *via* a sustained synthesis of NADPH. Consistent with this, the inhibition of the respiratory chain results in the reduction of the plastoquinone pool even under aerobic conditions [5]. Accordingly, the simplest interpretation of our (and others’) results is a model where the NADPH pool is submitted to two electron influx mechanisms, the utilization of reserves or carbohydrate catabolism and the photochemical PSI activity; and two efflux pathways, the Calvin cycle and the PQ reduction pathway, or cyclic pathway [13]. The efflux through the Calvin pathway requires ATP, and if we neglect the import of ATP from the mitochondrion [8], this route will be blocked in the dark. Under such circumstance, the electron influx resulting from carbohydrate catabolism goes into the PQ pool (Ndh pathway) and thence to the chloroplast oxidase. As stated above, under dark aerobic conditions, this oxidase is efficient enough to maintain a large fraction of the PQ pool in the oxidized state. On the other hand, under illumination specific to PSI, electrons are drained from the PQ pool, shunting the oxidase pathway [20].

Despite the influx of reducing power into the stroma, a fraction of P<sub>700</sub><sup>+</sup> still accumulates in the light, even in the mutants lacking Rubisco or ATPase where the consumption of electrons by the Calvin cycle cannot compensate for this entry of electrons. To account for this observation one may consider either a remaining slow electron

outflow, towards O<sub>2</sub> for example (Mehler reaction), or a decrease of the influx of reducing power as the concentration of NADPH in the stroma increases.

#### 4.2. The origin of the P<sub>700</sub><sup>+</sup> overshoot

On a dark to light transition, the flux towards the oxidase is diminished or interrupted because of the rerouting towards PSI [20]. Furthermore, if the light intensity is strong enough, the stock of electrons which was present in the PSI donors becomes displaced to NADPH, thereby enhancing the cyclic transfer rate, which depends on the reductive pressure exerted by the NADPH pool. This picture could provide a likely interpretation for the transient overshoot of P<sub>700</sub><sup>+</sup> that we observed during the early seconds of illumination. We suggest that the electron entry from NADPH into the PQ pool is initially slow because of the limited amount of electrons available. This amount increases steadily, however, because of the continuing supply of electrons from the carbohydrate catabolism, while the former draining route towards the thylakoid oxidase is now bypassed. This corresponds to the 0.5–4 s phase during which the level of P<sub>700</sub><sup>+</sup> decreases, reflecting the accelerated electron entry caused by increased reductive pressure from NADPH. This phase does not vary significantly when the illumination intensity is changed (see Fig. 4, black and red curves), as expected if this phenomenon is controlled by a light-independent mechanism.

An alternative – not necessarily exclusive – to the simple competition model described above is the possibility that the illumination somehow triggers an acceleration of the electron influx rate. The fact that a small overshoot still persists in the presence of MV (Fig. 7) might be an indication that such a process is operative. Previous literature dealing with the metabolism of algae reported the existence of an efficient photo-induced assimilation of acetate [27], insensitive to DCMU and stimulated by PSI excitation >720 nm [28]. On the one hand, it is consistent with the present finding of a sustained inflow of reducing power from carbohydrates catabolism, and on the other hand, it suggests that this inflow rate varies with illumination. Inasmuch as cyclic electron flow is coupled to proton translocation and ATP synthesis, one may assume the existence of an autocatalytic process: cyclic flow generates ATP, which induces acetate assimilation, produces NAD(P)H (*via* the Krebs cycle) which in turn is imported into the chloroplast and stimulates cyclic electron flow. Clearly, however, this mechanism cannot be the principal origin of the overshoot, since a pronounced activation of cyclic flow is still observed in the mutant devoid of chloroplast ATPase (Fig. 4).

#### 4.3. The cyclic electron flow rate in various circumstances

The cyclic flow rate of 10–15 e<sup>-</sup> s<sup>-1</sup> PSI<sup>-1</sup> found in the present work is somewhat faster than that reported by Maxwell and Biggins [23] (~5 e<sup>-</sup> s<sup>-1</sup> PSI<sup>-1</sup>) for various algal strains (in conditions similar to ours as regards PSII inhibition and aerobiosis). These authors believed that this “low” rate was not consistent with a significant contribution of the cyclic flow to photosynthesis. This issue should be reconsidered, however, taking into account the stoichiometric requirement of 3 ATP per 2 NADPH. For a dark-adapted sample, the electron flow rate of the photosynthetic chain at the onset of a strong continuous illumination is about 300 e<sup>-</sup> s<sup>-1</sup>, but under steady-state illumination, when the lumenal pH is acidified, it decreases down to 150 e<sup>-</sup> s<sup>-1</sup> [29,30]. This is partly due to the membrane potential, which opposes electron flow, and to the limitations of the enzyme reactions downstream of PSI, *i.e.* the Calvin cycle and availability of CO<sub>2</sub>. Moreover, numerous quenching mechanisms have been reported to further reduce the linear electron transport rate (non-photochemical quenching, state transitions, photoinhibition, etc...). In his review [1], Allen draws a unified picture of cyclic and non cyclic photosynthesis where 1 electron in 9 must be recycled, the other 8 being transferred linearly through 4



turnovers of PSII and PSI for the storage of 2 NADPH molecules (see Fig. 1). The overall process leads to the translocation of 14 protons, which is enough for the synthesis of 3 ATP, and 2 NADPH molecules, thereby matching the Calvin cycle stoichiometric requirement. The figure of 14 protons per 3 ATP molecules relies on the number (14) of c-subunits in the CF<sub>0</sub> ring of the ATPase, as found in higher plants [31]. This assumes the absence of any “proton slip” that would increase the proton requirement. One should also note that the c-subunit stoichiometry may be 13 in algae [32] and 15 in the cyanobacterium *Spirulina platensis* [33]. Conservatively, we retain the range 13–15 as the number of protons required for synthesizing 3 ATPs. Assuming an overall steady-state flow of  $150 \text{ e}^- \text{ s}^{-1}$ , the cyclic pathway should thus turn over at a rate of  $16\text{--}18 \text{ e}^- \text{ s}^{-1}$  ( $150/9 = 16.7$  for  $14 \text{ H}^+ / 3 \text{ ATP}$ ).

The figure of  $10\text{--}15 \text{ s}^{-1}$  found in our experiments with inhibited PSII, does not quite meet the above requirement, although not very far from it. However, in the present conditions, the cyclic rate is limited by the modest reductive pressure exerted by the stromal pool (NADPH), which depends on the slow electron influx from the catabolism of reserves. On the other hand, when PSII is active, its contribution will readily increase the reduction level of the stromal pool and thence the cyclic flux. In the picture we propose, the stromal NADPH pool plays a central role as a hub for the various electronic routes: the input routes encompass the electrons delivered by PSI (cyclic and non cyclic pathways) and the metabolic influx; the output routes encompass the PQ reducing pathway (feeding the cyclic flow and/or the oxidase) and the Calvin process. The ATP/NADPH requirement of the Calvin cycle regulates the allocation of electrons between the linear and cyclic pathways, providing a major feed-back loop. Indeed, on the one hand, the cyclic pathway competes with the Calvin cycle by rerouting the consumption of NADPH while, on the other hand, cyclic flow also promotes the carbon fixation by providing the extra ATP needed. This mechanism implies a definite stoichiometric ratio between the two flows. When PSII is inhibited, as in the present experiments, the ratio between the two effluxes can be calculated as follows. Assuming that 13–15 PSI turnovers drive the synthesis of the 3 ATP molecules which are required for the Calvin cycle to consume 2 NADPH (4 electrons), one obtains a ratio of  $13/4 = 3.25$  to  $15/4 = 3.75$ . Thus, under such circumstances, the electron current “trapped” in the cyclic PSI pathway is expected to be about 3–4 fold larger than the overall net flux in the chloroplast from, supposedly, starch degradation, to CO<sub>2</sub> (re-) reduction. This estimate is consistent with the ratio of 3.3 obtained here between the rate measured in absence ( $10 \text{ e}^- \text{ s}^{-1}$ ) and presence ( $3 \text{ e}^- \text{ s}^{-1}$ ) of MV.

## Acknowledgments

The authors are indebted to Xenie Johnson for critical reading of the manuscript, and to Pierre Joliot and Laurent Cournac for useful discussions. Financial support from the CNRS is gratefully acknowledged.

## Appendix A. Supplementary data

Supplementary data associated with this article can be found, in the online version, at doi:10.1016/j.bbabi.2009.07.009.

## References

- [1] J.F. Allen, Cyclic, pseudocyclic and noncyclic photophosphorylation: new links in the chain, *Trends Plant Sci.* 8 (2003) 15–19.
- [2] M.R. Badger, A. Kaplan, J.A. Berry, Internal inorganic carbon pool of *Chlamydomonas reinhardtii*: evidence for a carbon dioxide-concentrating mechanism, *Plant Physiol.* 66 (1980) 407–413.
- [3] A.H. Mehler, Studies on reactions of illuminated chloroplasts. I. Mechanism of the reduction of oxygen and other Hill reagents, *Arch. Biochem.* 33 (1951) 65–77.
- [4] E.M. Josse, A.J. Simkin, J. Gaffe, A.M. Laboure, M. Kuntz, P. Carol, A plastid terminal oxidase associated with carotenoid desaturation during chromoplast differentiation, *Plant Physiol.* 123 (2000) 1427–1436.
- [5] P. Bennoun, Evidence for a respiratory chain in the chloroplast, *Proc. Natl. Acad. Sci. U. S. A.* 79 (1982) 4352–4356.
- [6] A.M. Lennon, P. Prommeenate, P.J. Nixon, Location, expression and orientation of the putative chlororespiratory enzymes, Ndh and IMMUTANS, in higher-plant plastids, *Planta* 218 (2003) 254–260.
- [7] R. Scheibe, NADP<sup>+</sup>-malate dehydrogenase in C<sub>3</sub>-plants: regulation and role of a light-activated enzyme, *Physiol. Plant.* 71 (1987) 393–400.
- [8] C. Lemaire, F.A. Wollman, P. Bennoun, Restoration of phototrophic growth in a mutant of *Chlamydomonas reinhardtii* in which the chloroplast atpB gene of the ATP synthase has a deletion: an example of mitochondria-dependent photosynthesis, *Proc. Natl. Acad. Sci. U. S. A.* 85 (1988) 1344–1348.
- [9] D.I. Arnon, M.B. Allen, F.R. Whatley, Photosynthesis by isolated chloroplasts, *Nature* 174 (1954) 394–396.
- [10] P. Mitchell, The protonmotive Q cycle: a general formulation, *FEBS Lett.* 59 (1975) 137–139.
- [11] P. Mitchell, Protonmotive redox mechanism of the cytochrome *b-c1* complex in the respiratory chain: protonmotive ubiquinone cycle, *FEBS Lett.* 56 (1975) 1–6.
- [12] G. Peltier, L. Cournac, Chlororespiration, *Annu. Rev. Plant Biol.* 53 (2002) 523–550.
- [13] F. Jans, E. Mignolet, P.A. Houyoux, P. Cardol, B. Ghysels, S. Cuine, L. Cournac, G. Peltier, C. Remacle, F. Franck, A type II NAD(P)H dehydrogenase mediates light-independent plastoquinone reduction in the chloroplast of *Chlamydomonas*, *Proc. Natl. Acad. Sci. U. S. A.* 105 (2008) 20546–20551.
- [14] D. Rumeau, N. Becuwe-Linka, A. Beyly, M. Louwagie, J. Garin, G. Peltier, New subunits NDH-M, -N, and -O, encoded by nuclear genes, are essential for plastid Ndh complex functioning in higher plants, *Plant Cell* 17 (2005) 219–232.
- [15] D.I. Arnon, R.K. Chain, Regulation of ferredoxin-catalyzed photosynthetic phosphorylations, *Proc. Natl. Acad. Sci. U. S. A.* 72 (1975) 4961–4965.
- [16] J.P. Woessner, A. Masson, E.H. Harris, P. Bennoun, N.W. Gillham, J.E. Boynton, Molecular and genetic analysis of the chloroplast ATPase of *Chlamydomonas*, *Plant Mol. Biol.* 3 (1984) 177–190.
- [17] R.J. Spreitzer, G. Thow, G. Zhu, Pseudoreversion substitution at large-subunit residue 54 influences the CO<sub>2</sub>/O<sub>2</sub> specificity of chloroplast ribulose-bisphosphate carboxylase/oxygenase, *Plant Physiol.* 109 (1995) 681–685.
- [18] G. Thow, G. Zhu, R.J. Spreitzer, Complementing substitutions within loop regions 2 and 3 of the alpha/beta-barrel active site influence the CO<sub>2</sub>/O<sub>2</sub> specificity of chloroplast ribulose-1, 5-bisphosphate carboxylase/oxygenase, *Biochemistry* 33 (1994) 5109–5114.
- [19] R. Kuras, F.A. Wollman, The assembly of cytochrome b6/f complexes: an approach using genetic transformation of the green alga *Chlamydomonas reinhardtii*, *EMBO J.* 13 (1994) 1019–1027.
- [20] L. Cournac, G. Latouche, Z. Cerovic, K. Redding, J. Ravelin, G. Peltier, *In vivo* interactions between photosynthesis, mitorespiration, and chlororespiration in *Chlamydomonas reinhardtii*, *Plant Physiol.* 129 (2002) 1921–1928.
- [21] P. Joliot, A. Joliot, Quantification of cyclic and linear flows in plants, *Proc. Natl. Acad. Sci. U. S. A.* 102 (2005) 4913–4918.
- [22] I.D. Kuntz, M. Calvin, Kinetic studies of the two light reactions in photosynthesis, *Photochem. Photobiol.* 4 (1965) 537–548.
- [23] P.C. Maxwell, J. Biggins, Role of cyclic electron transport in photosynthesis as measured by the photoinduced turnover of P700 in vivo, *Biochemistry* 15 (1976) 3975–3981.
- [24] P. Tapie, Y. Choquet, J. Breton, P. Delepelaire, F.A. Wollman, Orientation of photosystem-I pigments. Investigation by low-temperature linear dichroism and polarized fluorescence emission, *Biochim. Biophys. Acta, Bioenerg.* 767 (1984) 57–69.
- [25] L. Bulté, P. Gans, F. Rebéillé, F.-A. Wollman, ATP control on state transitions *in vivo* in *Chlamydomonas reinhardtii*, *Biochim. Biophys. Acta, Bioenerg.* 1020 (1990) 72–80.
- [26] P. Joliot, D. Béal, A. Joliot, Cyclic electron flow under saturating excitation of dark-adapted Arabidopsis leaves, *Biochim. Biophys. Acta* 1656 (2004) 166–176.
- [27] E.G. Pringsheim, W. Wiessner, Photo-assimilation of acetate by green organisms, *Nature* 188 (1960) 919–921.
- [28] W. Wiessner, Quantum requirement for acetate assimilation and its significance for quantum measurements in photophosphorylation, *Nature* 205 (1965) 56–57.
- [29] G. Finazzi, F. Rappaport, *In vivo* characterization of the electrochemical proton gradient generated in darkness in green algae and its kinetic effects on cytochrome *b<sub>6</sub>f* turnover, *Biochemistry* 37 (1998) 9999–10005.
- [30] D.M. Kramer, C.A. Sacksteder, J.A. Cruz, How acidic is the lumen? *Photosynth. Res.* 60 (1999) 151–163.
- [31] H. Seelert, A. Poetsch, N.A. Dencher, A. Engel, H. Stahlberg, D.J. Muller, Structural biology. Proton-powered turbine of a plant motor, *Nature* 405 (2000) 418–419.
- [32] J.M. Meyer Zu Tittingdorf, S. Rexroth, E. Schafer, R. Schlichting, C. Giersch, N.A. Dencher, H. Seelert, The stoichiometry of the chloroplast ATP synthase oligomer III in *Chlamydomonas reinhardtii* is not affected by the metabolic state, *Biochim. Biophys. Acta* 1659 (2004) 92–99.
- [33] D. Pogoryelov, C. Reichen, A.L. Klyszzejko, R. Brunisholz, D.J. Muller, P. Dimroth, T. Meier, The oligomeric state of c rings from cyanobacterial F-ATP synthases varies from 13 to 15, *J. Bacteriol.* 189 (2007) 5895–5902.